

Origins of the Stereoselectivity in a Thiourea–Primary Amine-Catalyzed Nazarov Cyclization

Austin H. Asari,^{†,||} Yu-hong Lam,^{†,||} Marcus A. Tius,^{‡,§} and K. N. Houk^{*,†}

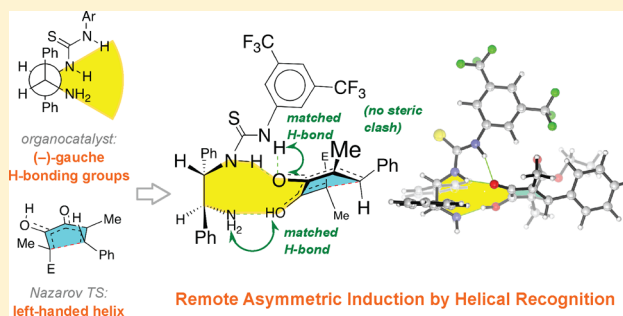
[†]Department of Chemistry and Biochemistry, University of California, Los Angeles, California 90095-1569, United States

[‡]Department of Chemistry, University of Hawaii at Manoa, Honolulu, Hawaii 96822, United States

[§]The Cancer Research Center of Hawaii, Honolulu, Hawaii 96813, United States

Supporting Information

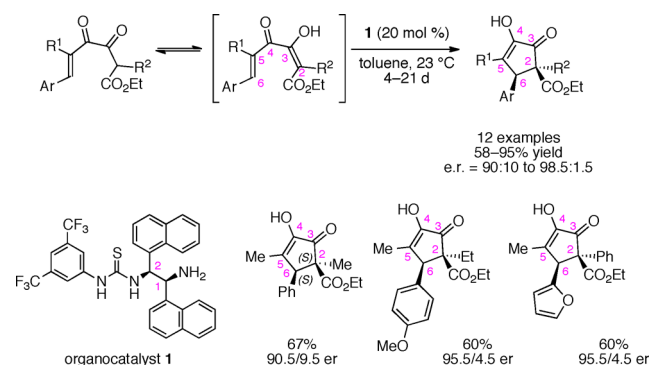
ABSTRACT: The origins of stereoselectivity of the Nazarov reactions of α -hydroxydivinylketones catalyzed by a vicinal thiourea–primary amine first reported by Tius have been explored with density functional theory. The electrocyclization transition structures in which the thiourea group of the catalyst donates two hydrogen bonds to the keto carbonyl group of the Nazarov reactant and the primary amine accepts a hydrogen bond from the hydroxyl group of the reactant have been modeled. The enantiomeric Nazarov transition structures, which are conventionally described by the absolute sense of conrotation of the dienone termini (“clockwise” or “counterclockwise”) in the literature, are nonplanar and adopt helically chiral conformations. The interactions of these helical electrocyclization transition structures with the chiral catalyst are studied in detail. The organocatalyst is found to employ a combination of hydrogen bonding and steric effects to achieve helical recognition of the Nazarov transition state.



INTRODUCTION

The Nazarov cyclization, a cationic 4π conrotatory electrocyclic reaction, is a general method for the synthesis of substituted cyclopentenones.^{1,2} Interest in the Nazarov cyclization has surged recently due to the realization that high levels of enantioselectivity can be achieved with the use of chiral auxiliaries³ or chiral Lewis acid or Brønsted acid catalysts.^{4,5} In 2010, Tius identified the novel vicinal thiourea–primary amine **1** as a highly enantioselective organocatalyst for the asymmetric Nazarov reaction of substituted divinylketones derived by tautomerization of α -ketoenones with 58–95% yield and 90:10 to 98.5:1.5 enantiomeric ratios (Scheme 1).⁵

Scheme 1. Tius's Organocatalytic Nazarov Reactions



Catalytic enantioselective Nazarov reactions have been developed primarily through the use of transition-metal complexes.² Besides Tius's thiourea–primary amine **1**, only a handful of organocatalysts are known to date to catalyze Nazarov reactions with high enantioselectivities, including BINOL-derived *N*-triflylphosphoramides as first reported by Rueping in 2007^{4a} and subsequently by Tius in 2014,^{4e} as well as a cinchona alkaloid derivative, reported by Frontier in 2015.⁶ Although numerous computational studies on the Nazarov cyclization are available,⁷ no structurally well-defined stereochemical models have been proposed for any organocatalytic variants of this reaction.⁸ It has been more challenging to develop enantioselective catalysts for electrocyclic ring-closing reactions than for other common pericyclic reactions.⁹ The first catalytic enantioselective Nazarov reaction was reported only in 2003.^{2a} For Tius's Nazarov reactions (Scheme 1), both the primary amine and the thiourea functional groups of **1** were found to be essential for reactivity and stereoselectivity,⁵ suggesting a bifunctional mode of activation of the divinylketone for cyclization.¹⁰ However, the mechanism by which chirality is transmitted from the remote stereocenters of **1** to the forming C–C bond upon cyclization is unknown. We undertook a computational investigation of the mechanism and origins of stereoselectivity for Tius's organocatalytic Nazarov reactions (Scheme 1). We demonstrate how the helically chiral

Received: August 24, 2015

Published: October 1, 2015

Nazarov transition state and the chiral catalyst are complementary in the favored transition state, interacting by a combination of hydrogen bonding and steric interactions.

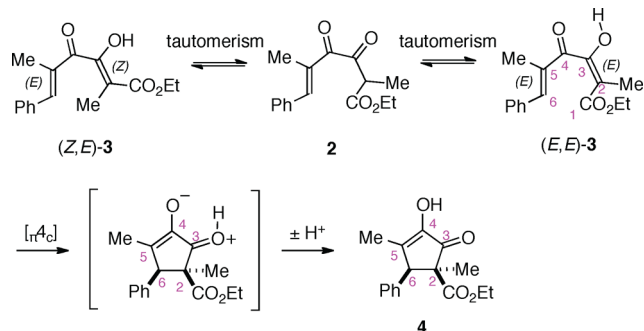
COMPUTATIONAL METHODS

Quantum mechanical calculations were performed using *Gaussian 09*.¹¹ The geometries were optimized using the M06-2X density functional¹² with the 6-31G(d) basis set. All of the optimized geometries were confirmed by frequency calculations to be minima (zero imaginary frequencies) or transition structures (a single imaginary frequency). Single-point energy calculations on the optimized geometries were performed using the M06-2X density functional and the polarized, triple- ζ valence quality def2-TZVPP basis set of Weigend and Ahlrichs.¹³ The thermal corrections evaluated from the unscaled vibrational frequencies at the M06-2X/6-31G(d) level on the optimized geometries were then added to the M06-2X/def2-TZVPP electronic energies to obtain the free energies. The free energy corrections were calculated using Truhlar's quasiharmonic approximation,¹⁴ where all of the real harmonic vibrational frequencies that are lower than 100 cm^{-1} are set to 100 cm^{-1} .

RESULTS AND DISCUSSION

The mechanism of the uncatalyzed Nazarov reaction is sketched in *Scheme 2*. Two isomers of enol **3** differing in the

Scheme 2. Mechanism of Nazarov Reaction



geometry of the enolic C=C double bond are possible from the tautomerism of α -ketoester **2**. Only cyclopentenones with cis stereochemistry with respect to the phenyl and the ester groups were experimentally observed,⁵ indicating that a conrotatory process had taken place only from the (E,E) enol. The ring-closed oxyallyl cation undergoes proton transfer between the two oxygen atoms on C3 and C4 during or after cyclization to give the α -hydroxycyclopentenone **4** as the final product. The stereochemistry of **4** is controlled by the structure of **3** and the stereoselectivity of the electrocyclic ring-closing step.

1. Control of Relative Configuration in Nazarov Cyclization. With respect to α -ketoester **2**, tautomerization to either enol isomer is endergonic by at least 0.7 kcal/mol, in agreement with the experimental observation that the enol form is a minor component at equilibrium (2:3 = 85:15).⁵ As shown in *Figure 1*, (E,E)-3 prefers to adopt the s-trans/s-trans conformation, while (Z,E)-3 prefers to adopt the s-trans/s-cis conformation. (Z,E)-3 is thermodynamically more stable than (E,E)-3 by 0.9 kcal/mol, primarily because the intramolecular hydrogen bond between the hydroxyl group and a carbonyl group forms a six-membered ring in (Z,E)-3 but a five-membered ring in (E,E)-3.¹⁵

The computed transition structures for the uncatalyzed Nazarov reactions for the (E,E) and (Z,E) isomers of **3** (TS-5a

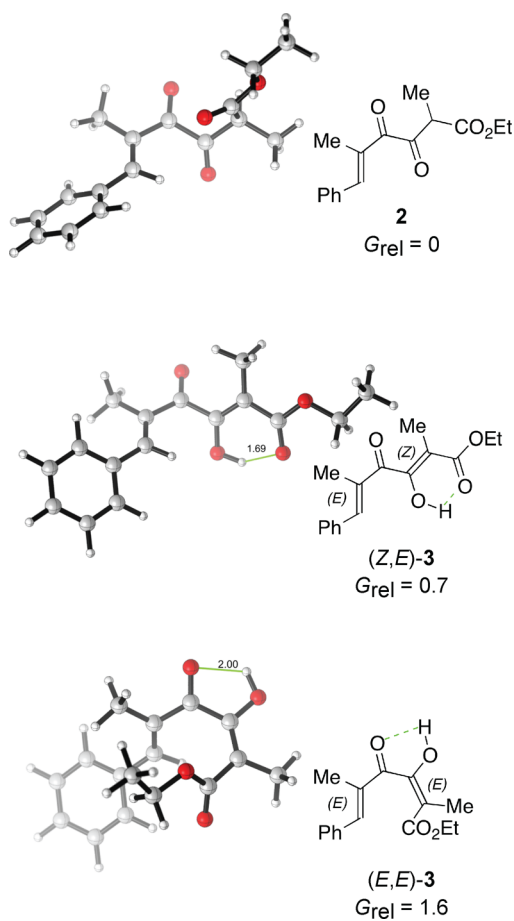


Figure 1. Computed structures and energies of **2**, (Z,E)-3, and (E,E)-3.

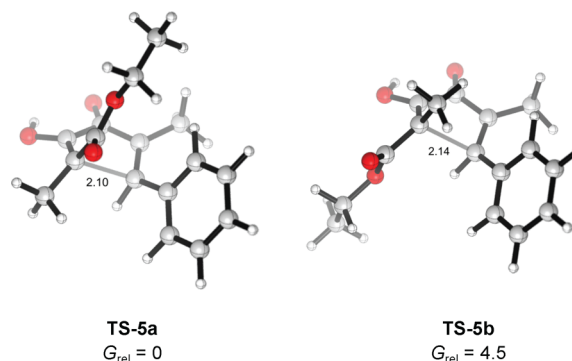


Figure 2. Conrotatory ring-closing transition structures for the uncatalyzed Nazarov cyclization of (E,E)-3 (TS-5a) and (Z,E)-3 (TS-5b).

and TS-5b, respectively) are shown in *Figure 2*. The free energy of activation for the uncatalyzed electrocyclicization is 37.1 kcal/mol for (Z,E)-3 and 31.7 kcal/mol for (E,E)-3. Since TS-5a is higher in energy than TS-5b by 4.5 kcal/mol, the Nazarov reaction from the Z enol does not compete kinetically with the reaction from the E enol, in accord with experimental findings.⁵

The energy difference between TS-5a and TS-5b is electronic in origin and can be explained by the theory of torquoselectivity in electrocyclic reactions.^{16,17} In the electrocyclic ring-opening reactions of cyclopentenyl cations¹⁷ and retro-Nazarov reactions,^{7c,g} or in the corresponding ring

closures, an electron-donating substituent prefers to be on the outside to minimize the filled–filled orbital interactions between the donor orbital and the σ orbital of the partially broken or formed σ bond. Electron-accepting groups, on the other hand, have a smaller outward preference or even favor the inside in order to maximize favorable overlap of the empty π^* orbital of the substituent and the HOMO of the partially formed bond. In both TS-5a and TS-5b, the large electron-donating phenyl group is outside. At the cyclization transition state of (*E,E*)-3 (TS-5a), the ester group is inside and the methyl group is outside. TS-5b is higher in energy because the *Z* configuration of the enol C=C double bond means that the methyl group is inside and the ester group is outside, arrangements that are disfavored compared to TS-5a.

The organocatalyzed Nazarov reaction reported by Tius (Scheme 1) was then investigated. For computational tractability the naphthyl rings on the optimal catalyst 1 were replaced by phenyl rings (6). This replacement was shown experimentally to only slightly reduce the enantiomeric ratio for the formation of (*S,S*)-4 from 90.5:9.5 ($\Delta\Delta G^\ddagger = 1.3$ kcal/mol) to 86.5:13.5 ($\Delta\Delta G^\ddagger = 1.1$ kcal/mol); the sense of asymmetric induction is unaffected.⁵

2. Conformations of the Organocatalyst. Figure 3 shows four conformers of 6 differing in the rotameric state of

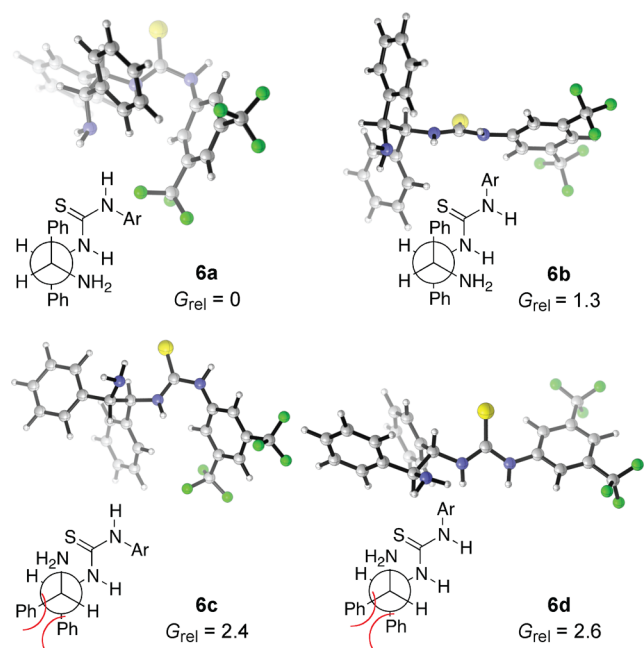


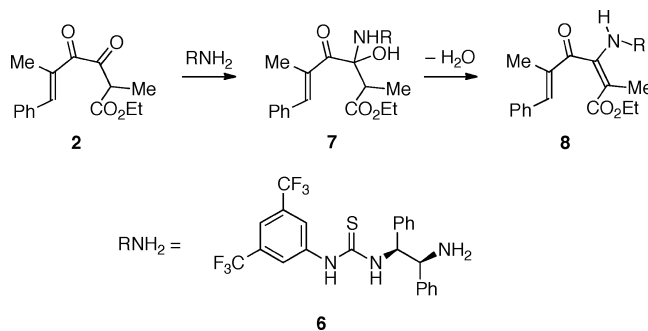
Figure 3. Conformations of organocatalyst 6 (M06-2X/def2-TZVPP//M06-2X/6-31G(d)). The relative free energies, G_{rel} , are given in kcal/mol. Ar = 3,5-(CF₃)₂C₆H₃.

the thiourea and the C1–C2 bond. Conformer 6a, in which the phenyl groups are antiperiplanar and the thiourea N–H bonds are anti, is the most stable, while the corresponding conformer 6b, in which the thiourea N–H bonds are syn and bidentate coordination is possible, is only 1.3 kcal/mol higher in energy. In 6a and 6b, the thiourea and the primary amine groups are (–)-gauche due to the absolute configuration of 6. The populations of conformations 6c and 6d, in which the two functional groups are (+)-gauche, are negligible, since these are 2.4 and 2.6 kcal/mol less stable than 6a, respectively, due to steric clash between the synclinal phenyl groups. Thus, the

(–)-gauche arrangement of the primary amine and thiourea groups forms a chiral binding pocket of 6 that is conformationally rather rigid.

3. Mechanism of the Catalyzed Reaction. At the outset of our studies, we explored whether the thiourea–primary amine catalyst 6 could induce torquoselectivity via an enamine intermediate (Scheme 3). The primary amine of catalyst 6

Scheme 3. Potential Enamine Nazarov Cyclization Route



would undergo nucleophilic addition into the C-3 carbonyl group of 2 to generate carbinolamine 7. Subsequent dehydration would generate 8, which can undergo the Nazarov cyclization. In the absence of an acid cocatalyst, the dehydration step is known to be the rate-determining step. Various computational and experimental studies have been conducted on the mechanistic details of enamine formation,¹⁸ although the intrinsic difficulties in the theoretical treatments of such reactions have recently been pointed out by Singleton.¹⁹ Hall and Smith used ab initio methods to investigate the bimolecular addition reaction between methylamine and formaldehyde and found the rate-determining dehydration step to possess a high energy barrier of 55.3 kcal/mol.^{18g} Upon inclusion of two explicit water molecules, this barrier is drastically lowered to 26.7 kcal/mol. Similarly, Patil and Sunoj used ab initio and DFT methods to study the cocatalyst “assisted” enamine formation between dimethylamine and propanal.^{18k} They found that two explicit methanol molecules lowered the dehydration barrier by as much as 16.7 kcal/mol in comparison to the simple bimolecular reaction. The incorporation of polar cocatalysts in these reactions is crucial in promoting enamine formation, as it both stabilizes the developing charge in the addition and dehydration step and facilitates an eight-membered relay proton transfer mechanism. Because no acid or other polar cocatalysts were included and the reaction was run in toluene for Tius’s Nazarov cyclization,⁵ these findings provide strong evidence that a mechanism involving an enamine intermediate cannot compete against the hydrogen-bonding catalysis described later. Furthermore, Tius and co-workers could not establish a catalytic cycle employing chiral diamine-triflic acid salts for the Nazarov cyclizations of α -hydroxydivinylketones due to the formation of a stable covalent intermediate resulting in complete product inhibition.²⁰ The addition of a strong acid was required to fully liberate the diamine from the cyclopentenone product. The organocatalyzed Nazarov reactions in Scheme 1 are slow due to product inhibition. Most likely the catalyst engages the product, an α -hydroxyketone, in the same way as it engages the starting material, which is also an α -hydroxyketone. Thus, we focus on the hydrogen-bonded mechanism rather than the enamine mechanism.

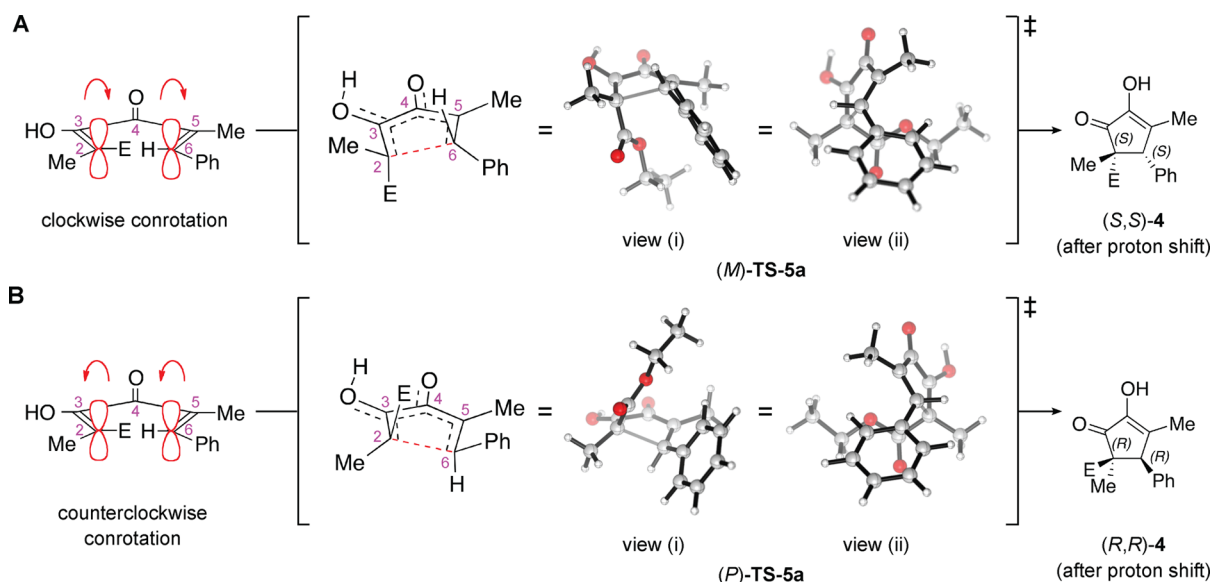


Figure 4. Nazarov transition structures TS-5a of the *M* (A) and the *P* (B) helicity.

The 4π electrocyclozation is expected to be the rate-determining and stereocontrolling step. We assumed that keto–enol tautomerization is a relatively low free energy barrier process and the interconversion between the hydrogen-bonded complexes of enols (*Z,E*)-3 and (*E,E*)-3 is rapid. The product distribution would then follow the Curtin–Hammett principle; that is, the relative transition state free energies determine the product distribution. In support of this assumption, Pápai and co-workers conducted DFT calculations on the enantioselective Michael addition of acetylacetone to a nitroolefin catalyzed by Takemoto’s bifunctional thiourea catalyst.²¹ They found that proton transfer from coordinated acetylacetone to the tertiary amine of the thiourea catalyst has a relatively low energy barrier. The similarities in both the substrate and catalyst we investigate with these studies support our assumption that the free energy barrier for keto–enol tautomerization is much lower than the free energy barrier for electrocyclozation.

4. Control of Absolute Configuration in Nazarov Cyclization Catalyzed by 6. The dienone chains in the reactant (*E,E*)-3 (Figure 1) and the Nazarov transition state (Figure 2) are nonplanar but adopt helically chiral conformations.²² This helicity is a natural consequence of the conrotatory nature of the transition state and occurs to enable overlap of the top face of the π system at one terminus with the bottom face at the other terminus. The sense of helicity of the Nazarov transition state dictates the absolute configuration of the oxyallyl cation and the cyclopentenone product 4. As shown in Figure 4, clockwise conrotation, which leads to the (*S,S*) cyclopentenone, displays the left-handed or *M* helical conformation. Counterclockwise conrotation, which leads to the (*R,R*) cyclopentenone, adopts the right-handed or *P* helical conformation. The enantiocontrol in a catalytic Nazarov reaction of divinylketones can be understood by considering how the chiral catalyst preferentially interacts with the transition structure with one helicity. In what follows, we show how the chiral pocket of 6, in which the thiourea and the primary amine are held at the (–)-gauche disposition, preferentially recognizes the *left*-handed (*M*) helical conformer at the Nazarov transition state to selectively catalyze the formation of the (*S,S*) enantiomer of 4.

The Nazarov reaction of (*E,E*)-3 catalyzed by 6 displays a bifunctional mode of activation in which the thiourea donates two hydrogen bonds to the keto carbonyl group and the primary amine accepts a hydrogen bond from the hydroxyl group. The formation of the hydrogen-bonded complexes from (*E,E*)-3 and 6 is endergonic by 0.9 to 3.4 kcal/mol.²³ We have computed the hydrogen-bonded complexes of CH_3OH and CH_3NH_2 . The complex $\text{CH}_3\text{O}-\text{H}\cdots\text{NH}_2\text{CH}_3$, in which the amine accepts the hydrogen bond, is 3.7 kcal/mol more stable than the alternative complex in which the alcohol serves as the acceptor. Thus, only transition structures in which the primary amine of 6 accepts a hydrogen bond from the enol OH and the thiourea coordinates to the keto carbonyl oxygen were studied.

A total of eight transition structures were located. These arise from two possible senses of helicity leading to enantiomeric products, two possible positions of the catalyst relative to the mean plane of the cyclizing moiety, and two possible conformations of the single bond linking the ester carbonyl group and the pentadienyl chain (*s-cis* or *s-trans*). The relative Gibbs energies of the eight transition structures are given in Table 1. The Gibbs energy of activation for the electrocyclozation through TS-9a, the lowest-energy TS, is 28.1 kcal/mol.

The four transition structures (TS-9a–TS-9d) that differ only in the sense of helicity and catalyst positioning are shown

Table 1. Relative Free Energies of Stereoisomeric Transition Structures TS-9 for Electrocyclozation of (*E,E*)-3

Transition Structure	$\Delta\Delta G^\ddagger$ (kcal/mol)
TS-9a	0
TS-9b	1.3
TS-9c	1.7
TS-9d	1.4
TS-9a' ^a	0.2
TS-9b' ^a	2.3
TS-9c' ^a	3.0
TS-9d' ^a	2.0

^aTS-9a'–TS-9d' are the same as TS-9a–TS-9d except for the *s-cis* or *s-trans* conformation of the ester with respect to the enone.

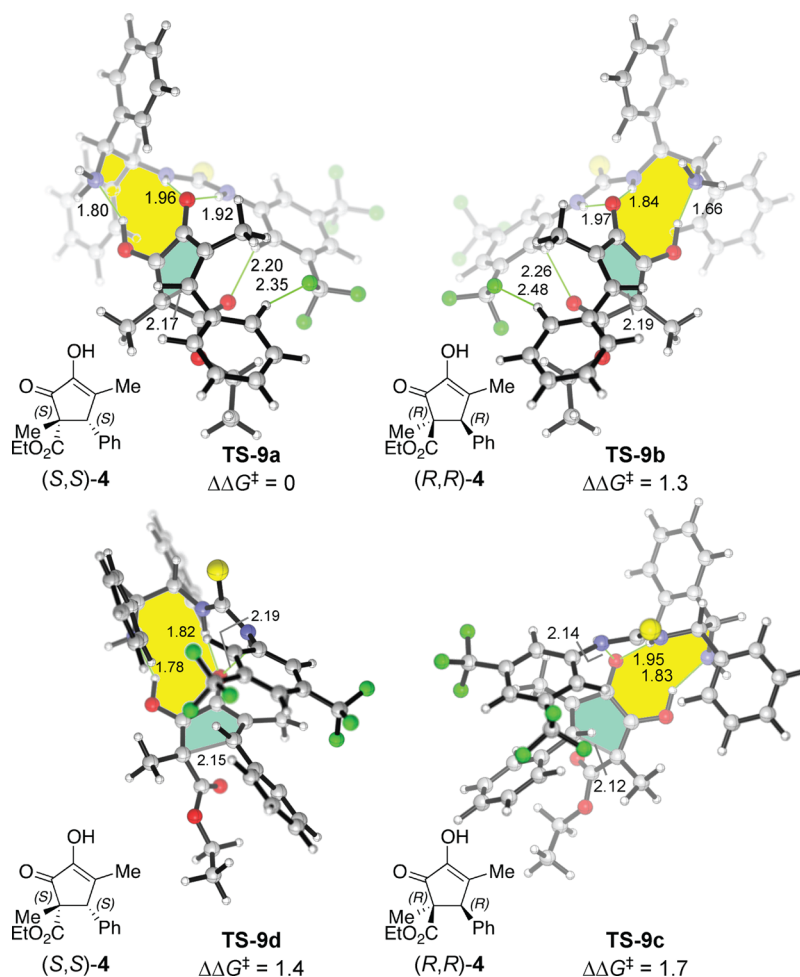


Figure 5. Transition structures TS-9a–TS-9d for electrocyclic ring closure of (*E,E*)-3 catalyzed by 6 (M06-2X/def2-TZVPP//M06-2X/6-31G(d)). The differences in free energy of activation are given in kcal/mol compared with TS-9a. The resulting cyclopentenone 4 for each transition structure is also shown. In each TS, the incipient five-membered ring and the hydrogen-bonded ring are colored in cyan and yellow, respectively.

in Figure 5. The keto carbonyl group of (*E,E*)-3 is coordinated by the thiourea group of 6 from the back in TS-9a and TS-9b, and from the front in TS-9c and TS-9d. The cyclizing moieties of TS-9a and TS-9d, which lead to (*S,S*)-4, are left-handed helices, while TS-9b and TS-9c, for the formation of (*R,R*)-4, contain right-handed helices. These transition structures are analyzed in more detail in the following sections.

TS-9a–TS-9d all contain the *s-cis* conformation with respect to the O–C1–C2–C3 bond; the *s-trans* transition structures (TS-9a'–TS-9d'), which are 0.2–1.3 kcal/mol higher in energy than the corresponding *s-cis* structures, are given in the Supporting Information (SI). The Gibbs energies of activation for the electrocyclizations of (*Z,E*)-3 with the catalysis of 6 are 5.2 kcal/mol or more higher than that for the electrocyclization of (*E,E*)-3 through TS-9a and, thus, do not contribute to cyclopentenone formation under the experimental conditions. This is consistent with the difference in reactivity between (*Z,E*)-3 and (*E,E*)-3 in the uncatalyzed electrocyclic ring closure (vide supra). The TSs for the catalyzed reactions of (*Z,E*)-3 are also given in the SI.

Six of the TSs are up to 2.0 kcal/mol higher in energy than TS-9a (Table 1). Taking the Boltzmann distribution of the relative Gibbs energies of the eight TSs yields a computed enantioselectivity of 91:9 in favor of the (*S,S*) enantiomer, in

good agreement with the sense and level of enantioselectivity experimentally observed with catalyst 6 (86.5:13.5).

Both TS-9a and TS-9d give rise to the (*S,S*) enantiomer of 4. TS-9d is 1.4 kcal/mol higher in free energy than TS-9a due to steric hindrance. The catalyst moiety of TS-9d is 1.8 kcal/mol higher in energy than the catalyst moiety of TS-9a. An overlay of TS-9a and TS-9d in which the dienone moieties are superimposed (Figure 6) shows that, in TS-9d, the catalyst *N*-aryl ring clashes with the substituents on the C5=C6 bond of the dienone. Such steric repulsion is absent in TS-9a. Instead, the *N*-aryl ring is involved in weak C–H...O and C–H...F attractions with the ester carbonyl group and the phenyl ring of the dienone, respectively (2.20 and 2.35 Å, Figure 5).

Both TS-9b and TS-9c give rise to the (*R,R*) enantiomer of 4. TS-9b is less stable than TS-9a by 1.3 kcal/mol. As shown by the Newman projections along the C1–C2 bond of the catalyst in Figure 7, the ten-membered hydrogen-bonded ring appears twisted in TS-9b but not in TS-9a. The two hydrogen bonds closing the ten-membered rings are shorter in TS-9b than in TS-9a, but this stabilization may be partially offset by secondary electrostatic repulsion²⁴ between the amine nitrogen and the keto oxygen (N2 and O2 in Figure 7), which are 0.31 Å closer in TS-9b than in TS-9a (N2–O2 distance = 3.52 Å in TS-9a, 3.21 Å in TS-9b). TS-9b is further disfavored by a more eclipsed N1–C1–C2–N2 dihedral angle (-48°) of the catalyst

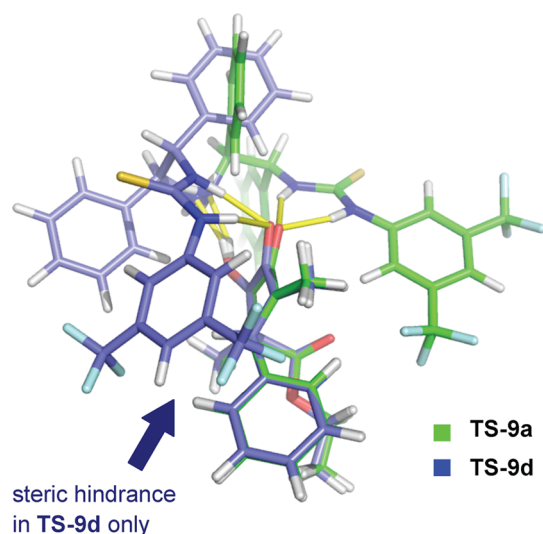


Figure 6. Overlay of TS-9a and TS-9d superimposing the dienone moieties. The steric clash between the *N*-aryl ring of **6** and the C5 and C6 substituents of (*E,E*)-**3** is indicated.

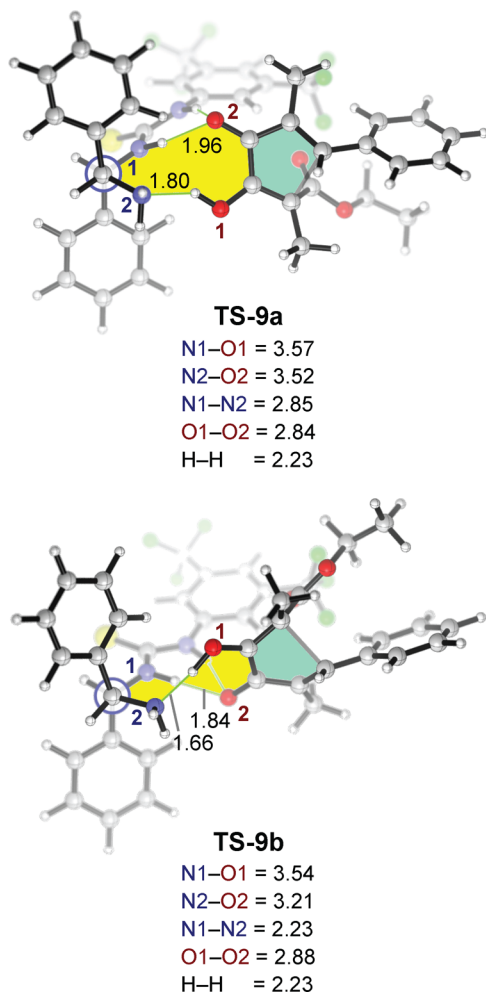


Figure 7. Newman projections of TS-9a and TS-9b along catalyst C1–C2 bond. The non-hydrogen-bonding distance for each pair of heteroatoms of the thiourea, amine, and the ketoenol groups, as well as the distance between the two H atoms engaged in the hydrogen bonds, is shown in angstroms.

moiety while the C1–C2 bond in TS-9a is ideally staggered (-61°). The catalyst moiety of TS-9b is 5.4 kcal/mol higher in energy than the catalyst moiety of TS-9a. Thus, the net destabilization of TS-9b results from an interplay of hydrogen bonding and catalyst distortion.

That the difference in energy of TS-9a and TS-9b is primarily due to the structure of the hydrogen-bonded rings can be seen from the overlay in Figure 8, which shows that the

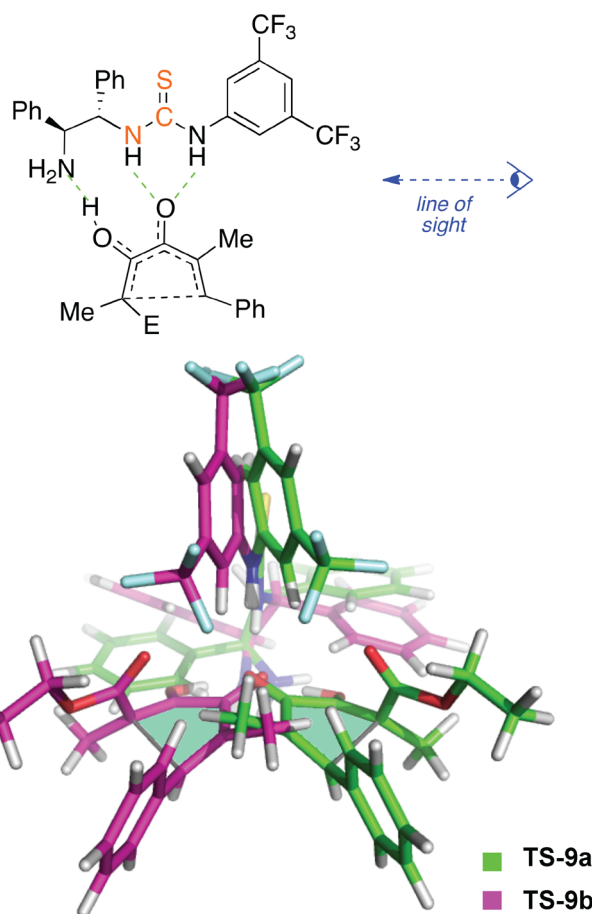


Figure 8. Overlay of TS-9a and TS-9b superimposing the orange atoms of the organocatalyst moiety. The incipient five-membered ring is color-filled with cyan.

dienone moiety and the *N*-aryl ring portion of the catalyst in TS-9a and TS-9b resemble a pair of mirror images. The steric interactions within these moieties are thus comparable between the two transition structures. Indeed, C–H \cdots O and C–H \cdots F attractions between the catalyst *N*-aryl ring and the reactant, analogous to those in TS-9a, are present in TS-9b (2.26 and 2.48 Å, Figure 5).

Why is the catalyst more eclipsed in TS-9b? Figure 9 shows TS-9a and TS-9b oriented with the C1–C2 bond of the catalyst vertical. In TS-9a, the catalyst thiourea group and the reactant carbonyl group are close to the viewer, while the catalyst amine and the reactant hydroxyl are located in the rear. Thus, the catalyst can interact with the reactant through hydrogen bonding without much catalyst distortion. Inverting the helicity of the cyclizing moiety, as in TS-9b, places the hydroxyl group at the front and the carbonyl group at the back. To maintain hydrogen bonding in this mismatched geometry, rotation about the C1–C2 bond of the catalyst occurs to move

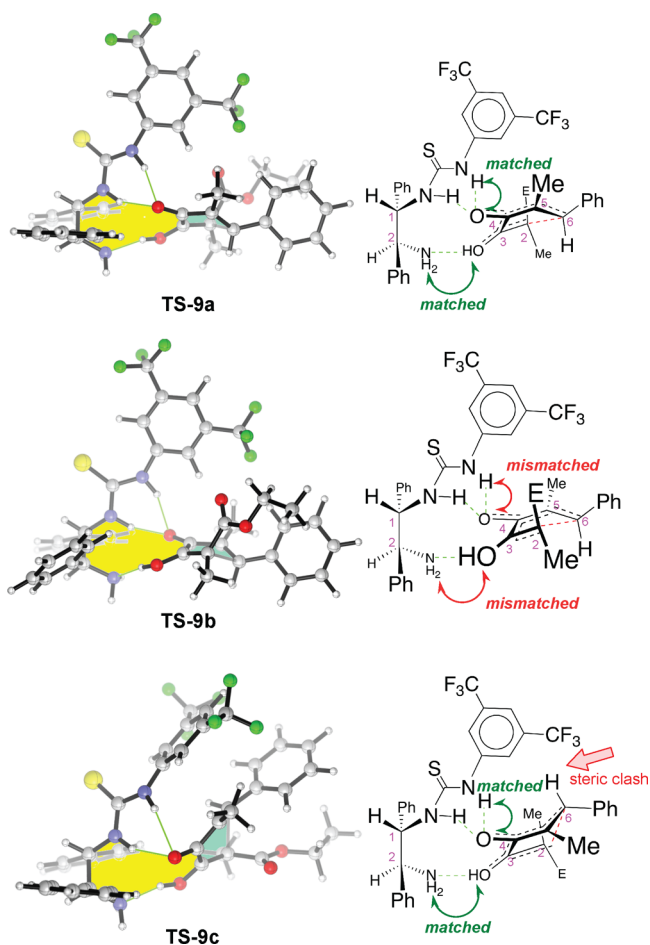


Figure 9. TS-9a–9c with the C1–C2 bond of the catalyst oriented vertically. In the schematic drawings, atoms closer to the viewer are represented by larger font sizes. E = CO₂Et.

the amine group toward the front and the thiourea group toward the back. Thus, the optimized geometry of TS-9b displays a smaller N1–C1–C2–N2 dihedral angle.

TS-9c, the alternative (*R,R*) TS, is 1.7 kcal/mol higher in energy than TS-9a. As shown by the Newman projection in Figure 10, the C1–C2 bond of the catalyst moiety of TS-9c is staggered. The hydrogen-bonded ring in TS-9c (Figure 10) possesses similar hydrogen-bond lengths (1.95 and 1.83 Å) and similar distances of separation between the non-hydrogen-bonded heteroatoms (Figure 7) compared to the hydrogen-bonded ring in TS-9a. The catalyst moiety of TS-9c also has a staggered (N1–C1–C2–N2 = –63°) conformation and is only 0.4 kcal/mol less stable than the catalyst moiety of TS-9a.

The similarities and differences between TS-9a and TS-9c can be visualized in Figure 11A, which overlays the geometries of the two transition structures. The blue box highlights the good geometrical agreement with respect to the vicinal diaryl portion of the catalyst and the keto–enol moiety of (*E,E*)-3 as a result of matched hydrogen bonding. The key difference between the two transition structures is boxed in pink. In TS-9c, the catalyst *N*-aryl group is tilted in order to alleviate steric clash with the substituents on the C5=C6 olefin of (*E,E*)-3. This steric repulsion, which is also found in TS-9d (vide supra), is readily apparent in Figure 11B, in which the catalyst moiety of TS-9a and the dienone moiety of TS-9c are overlaid without further geometry optimization. Because of this repulsion, the

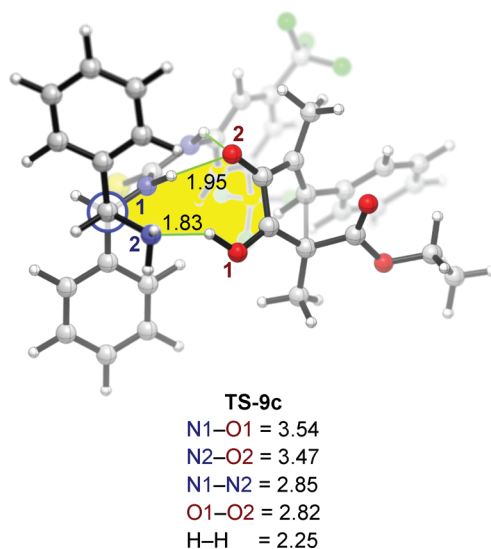


Figure 10. Newman projection of TS-9c sighted along the C1–C2 bond of the catalyst moiety. The non-hydrogen-bonding distance for each pair of heteroatoms of the thiourea, amine, and the ketoenol groups, as well as the distance between the two H atoms engaged in the hydrogen bonds, is shown in angstroms.

third hydrogen bond in TS-9c (i.e., the hydrogen bond from the thiourea N–H to the keto carbonyl outside the hydrogen-bonded ring) is significantly lengthened and weakened (2.14 Å in TS-9c vs 1.92 Å in TS-9a; Figure 5). As shown in Figure 9, both TS-9c and TS-9a feature the carbonyl and the hydroxyl groups of the Nazarov reactant in matched positions for hydrogen bonding with the catalyst. However, in TS-9c, the flap of the approximate envelope conformation of the dienone points upward toward the *N*-aryl ring of the catalyst, resulting in steric clash and destabilization.

CONCLUSIONS

The mechanism and the origins of diastereo- and enantioselectivity in the Nazarov reactions of α -hydroxydivinylketones ((*E,E*)-3) catalyzed by the vicinal thiourea–primary amine **6** have been elucidated computationally. The exclusive diastereoselectivity is due to the lower activation barrier of electrocyclization for the *E* enol (*E,E*)-3 than for the *Z* enol (*Z,E*)-3. At the electrocyclization transition state, (*E,E*)-3 places the phenyl and methyl groups outside and the ester carbonyl group inside.

The thiourea and the primary amine groups are held in a (–)-gauche disposition due to the antiperiplanar preference of the bulky phenyl rings on C1 and C2 of **6**. For the Nazarov reaction of (*E,E*)-3, the (*S,S*) enantiomer of **4** is formed via a transition structure in which the pentadienyl backbone is a left-handed (*M*) helix. Catalyst **6** is selective for the formation of (*S,S*)-**4** because the catalyst can maintain hydrogen bonding with the Nazarov TS in the left-handed helix conformation with less distortion while minimizing steric hindrance from its *N*-arylthiourea moiety, as shown in TS-9a. On the other hand, a right-handed helical transition state results in a twisted hydrogen-bonded complex (in TS-9b) or steric clash with the catalyst (in TS-9c). While the use of steric blocking groups is a prevalent paradigm in the design of enantioselective catalysts,^{1,2} TS-9a and TS-9b differ mainly in the conformation of the hydrogen-bonded ring with minimal differences in steric congestion involving the *N*-arylthiourea moiety of the catalyst.

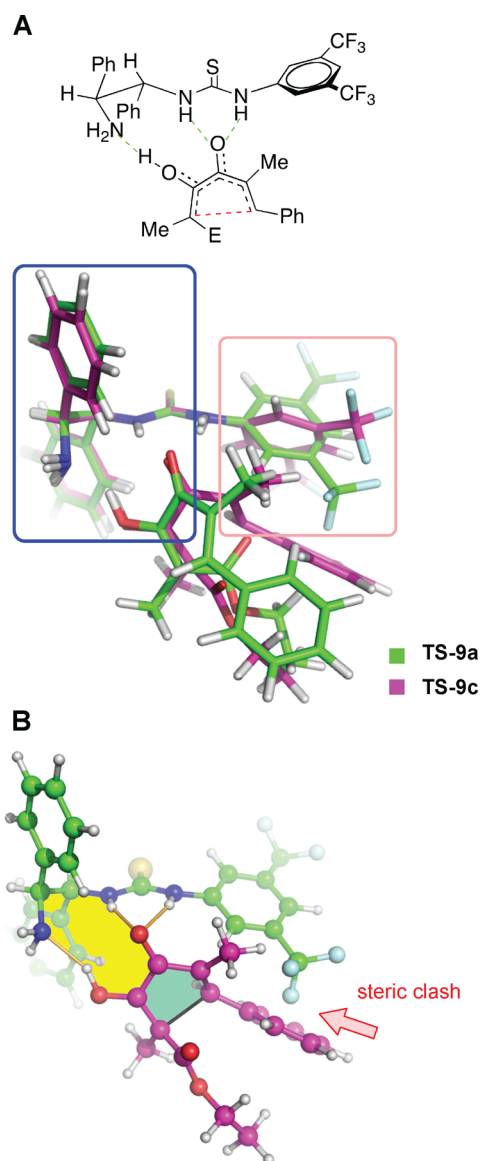


Figure 11. (A) Overlay of TS-9a and TS-9c. The similarity in conformation of the ten-membered hydrogen-bonded rings is highlighted in a blue box, while the different manner of tilting of the *N*-aryl ring of **6** is boxed in pink. E = CO₂Et. (B) Same overlay as (A), but showing only the catalyst moiety of TS-9a and the cyclizing moiety of TS-9c.

The Nazarov reactions of divinylketones pose a special challenge for enantioselective catalyst design because the catalyst must distinguish between the two possible helicities of the five-membered cyclic transition state entailing only small differences in torsion angles. The helical arrangement of the thiourea–amine is complementary to one of the helical transition states.

■ ASSOCIATED CONTENT

Supporting Information

The Supporting Information is available free of charge on the ACS Publications website at DOI: 10.1021/jacs.5b08969.

Electrocyclization transition structures for (*Z,E*)-**3** under the catalysis of **6**. Hydrogen-bonded complexes of (*E,E*)-**3** and **6**. Cartesian coordinates and thermodynamic parameters (in hartrees) of all stationary points (PDF)

■ AUTHOR INFORMATION

Corresponding Author

*houk@chem.ucla.edu

Author Contributions

||A.H.A. and Y.-h.L. contributed equally.

Notes

The authors declare no competing financial interest.

■ ACKNOWLEDGMENTS

We are grateful to the National Institute of General Medical Sciences, National Institute of Health (GM-36770 to K.N.H.) and the National Science Foundation (CHE-1361104) for financial support of this research. The computations were performed on the Hoffman2 cluster at UCLA and the Extreme Science and Engineering Discovery Environment (XSEDE), which is supported by the National Science Foundation (OCI-1053575).

■ REFERENCES

- (1) (a) Habermas, K. L.; Denmark, S. E.; Jones, T. K. *Org. React.* **1994**, *45*, 1–158. (b) Tius, M. A. *Acc. Chem. Res.* **2003**, *36*, 284–290. (c) Harmata, M. *Chemtracts* **2004**, *17*, 416–435. (d) Pellissier, H. *Tetrahedron* **2005**, *61*, 6479–6517. (e) Tius, M. A. *Eur. J. Org. Chem.* **2005**, *2005*, 2193–2206. (f) Frontier, A. J.; Collison, C. *Tetrahedron* **2005**, *61*, 7577–7606. (g) Grant, T. N.; Rieder, C. J.; West, F. G. *Chem. Commun.* **2009**, 5676–5688. (h) Nakanishi, W.; West, F. G. *Curr. Opin. Drug Discovery Dev.* **2009**, *12*, 732–751. (i) Vaidya, T.; Eisenberg, R.; Frontier, A. J. *ChemCatChem* **2011**, *3*, 1531–1548. (j) Shimada, N.; Stewart, C.; Tius, M. A. *Tetrahedron* **2011**, *67*, 5851–5870. (k) Schotes, C.; Mezzetti, A. *ACS Catal.* **2012**, *2*, 528–538. (l) Spencer, W. T., III; Vaidya, T.; Frontier, A. J. *Eur. J. Org. Chem.* **2013**, *2013*, 3621–3633. (m) Tius, M. A. *Chem. Soc. Rev.* **2014**, *43*, 2979–3002. (n) West, F. G.; Scadeng, O.; Wu, Y.-K.; Fradette, R. J.; Joy, S. The Nazarov Cyclization. In *Comprehensive Organic Synthesis II*, 2nd ed.; Knochel, P., Molander, G. A., Eds.; Elsevier: The Netherlands, 2014; Vol. 5, pp 827–866.
- (2) (a) Aggarwal, V. K.; Belfield, A. J. *Org. Lett.* **2003**, *5*, 5075–5078. (b) Liang, G.; Gradl, S. N.; Trauner, D. *Org. Lett.* **2003**, *5*, 4931–4934. (c) Liang, G.; Trauner, D. *J. Am. Chem. Soc.* **2004**, *126*, 9544–9545. (d) Nie, J.; Zhu, H. W.; Cui, H.; Hua, M.; Ma, J. *Org. Lett.* **2007**, *9*, 3053–3056. (e) Walz, I.; Togni, A. *Chem. Commun.* **2008**, 4315–4317. (f) Yaji, K.; Shindo, M. *Synlett* **2009**, *2009*, 2524–2528. (g) Kawatsura, M.; Kajita, K.; Hayase, S.; Itoh, T. *Synlett* **2010**, *2010*, 1243–1246. (h) Cao, P.; Deng, C.; Zhou, Y.-Y.; Sun, X.-L.; Zheng, J.-C.; Xie, Z.; Tang, Y. *Angew. Chem., Int. Ed.* **2010**, *49*, 4463–4466. (i) Hutson, G. E.; Türkmen, Y. E.; Rawal, V. H. *J. Am. Chem. Soc.* **2013**, *135*, 4988–4991. (j) Raja, S.; Nakajima, M.; Rueping, M. *Angew. Chem., Int. Ed.* **2015**, *54*, 2762–2765.
- (3) (a) Pridgen, L. N.; Huang, K.; Shilcrat, S.; Tickner-Eldridge, A.; DeBrosse, C.; Haltiwanger, R. C. *Synlett* **1999**, *1999*, 1612–1614. (b) Harrington, P. E.; Tius, M. A. *Org. Lett.* **2000**, *2*, 2447–2450. (c) Harrington, P. E.; Murai, T.; Chu, C.; Tius, M. A. *J. Am. Chem. Soc.* **2002**, *124*, 10091–10100. (d) Kerr, D. J.; Metje, C.; Flynn, B. L. *Chem. Commun.* **2003**, 1380–1381. (e) Dhoro, F.; Kristensen, T. E.; Stockmann, V.; Yap, G. P. A.; Tius, M. A. *J. Am. Chem. Soc.* **2007**, *129*, 7256–7257. (f) Banaag, A. R.; Tius, M. A. *J. Org. Chem.* **2008**, *73*, 8133–8141. (g) Kerr, D. J.; White, J. M.; Flynn, B. L. *J. Org. Chem.* **2010**, *75*, 7073–7084. (h) Kerr, D. J.; Miletic, M.; Chaplin, J. H.; White, J. M.; Flynn, B. L. *Org. Lett.* **2012**, *14*, 1732–1735. (i) Wu, Y.-K.; Niu, T.; West, F. G. *Chem. Commun.* **2012**, *48*, 9186–9188.
- (4) (a) Rueping, M.; Ieawsuwan, W.; Antonchick, A. P.; Nachtsheim, B. J. *Angew. Chem., Int. Ed.* **2007**, *46*, 2097–2100. (b) Rueping, M.; Ieawsuwan, W. *Adv. Synth. Catal.* **2009**, *351*, 78–84. (c) Rueping, M.; Ieawsuwan, W. *Chem. Commun.* **2011**, *47*, 11450–11452. (d) Raja, S.; Ieawsuwan, W.; Korotkov, V.; Rueping, M. *Chem. - Asian J.* **2012**, *7*,

2361–2366. (e) Jolit, A.; Walleser, P. M.; Yap, G. P. A.; Tius, M. A. *Angew. Chem., Int. Ed.* **2014**, *53*, 6180–6183.

(5) Basak, A. K.; Shimada, N.; Bow, W. F.; Vivic, D. A.; Tius, M. A. *J. Am. Chem. Soc.* **2010**, *132*, 8266–8267.

(6) Huang, Y.-W.; Frontier, A. J. *Tetrahedron Lett.* **2015**, *56*, 3523–3526.

(7) (a) Smith, D. A.; Ulmer, C. W., II *Tetrahedron Lett.* **1991**, *32*, 725–728. (b) Smith, D. A.; Ulmer, C. W., II *J. Org. Chem.* **1991**, *56*, 4444–4447. (c) Smith, D. A.; Ulmer, C. W., II *J. Org. Chem.* **1993**, *58*, 4118–4121. (d) Smith, D. A.; Ulmer, C. W., II *J. Org. Chem.* **1997**, *62*, 5110–5115. (e) Iglesias, B.; de Lera, A. R.; Rodríguez-Otero, J.; López, S. *Chem. - Eur. J.* **2000**, *6*, 4021–4033. (f) Nieto Faza, O.; Silva López, C.; Alvarez, R.; de Lera, A. R. *Chem. - Eur. J.* **2004**, *10*, 4324. (g) Harmata, M.; Schreiner, P. R.; Lee, D. R.; Kirchoefer, P. L. *J. Am. Chem. Soc.* **2004**, *126*, 10954. (h) Faza, O. N.; López, C. S.; Alvarez, R.; de Lera, A. R. *Chem. Commun.* **2005**, 4285–4287. (i) Cavalli, A.; Masetti, M.; Recanatini, M.; Prandi, C.; Guarna, A.; Occhiato, E. G. *Chem. - Eur. J.* **2006**, *12*, 2836–2845. (j) Shi, F.-Q.; Li, X.; Xia, Y.; Zhang, L.; Yu, Z.-X. *J. Am. Chem. Soc.* **2007**, *129*, 15503–15512. (k) Lemiere, G.; Gandon, V.; Cariou, K.; Fukuyama, T.; Dhimane, A.-L.; Fensterbank, L.; Malacria, M. *Org. Lett.* **2007**, *9*, 2207–2209. (l) Cavalli, A.; Pacetti, A.; Recanatini, M.; Prandi, C.; Scarpi, D.; Occhiato, E. G. *Chem. - Eur. J.* **2008**, *14*, 9292–9304. (m) Marcus, A. P.; Lee, A. S.; Davis, R. L.; Tantillo, D. J.; Sarpong, R. *Angew. Chem., Int. Ed.* **2008**, *47*, 6379–6383. (n) Cordier, P.; Aubert, C.; Malacria, M.; Lacôte, E.; Gandon, V. *Angew. Chem., Int. Ed.* **2009**, *48*, 8757. (o) Lemière, G.; Gandon, V.; Cariou, K.; Hours, A.; Fukuyama, T.; Dhimane, A.-L.; Fensterbank, L.; Malacria, M. *J. Am. Chem. Soc.* **2009**, *131*, 2993. (p) Faza, O. N.; López, C. S.; de Lera, A. R. *J. Org. Chem.* **2011**, *76*, 3791–3796. (q) Krafft, M. E.; Vidhani, D. V.; Cran, J. W.; Manoharan, M. *Chem. Commun.* **2011**, *47*, 6707. (r) Lebœuf, D.; Huang, J.; Gandon, V.; Frontier, A. J. *Angew. Chem., Int. Ed.* **2011**, *50*, 10981–10985. (s) González-Pérez, A. B.; Vaz, B.; Faza, O. N.; de Lera, A. R. *J. Org. Chem.* **2012**, *77*, 8733–8743. (t) Lebœuf, D.; Gandon, V.; Ciesielski, J.; Frontier, A. J. *J. Am. Chem. Soc.* **2012**, *134*, 6296–6308. (u) Lebœuf, D.; Theiste, E.; Gandon, V.; Daifuku, S. L.; Neidig, M. L.; Frontier, A. J. *Chem. - Eur. J.* **2013**, *19*, 4842–4848. (v) Flynn, B. L.; Manchala, N.; Krenske, E. H. *J. Am. Chem. Soc.* **2013**, *135*, 9156–9163. (w) Kitamura, K.; Shimada, N.; Atesin, A. C.; Ateşin, T. A.; Tius, M. A. *Angew. Chem., Int. Ed.* **2015**, *54*, 6288–6291.

(8) Rueping has performed DFT calculations to explain the absolute configurations of his Cu-catalyzed catalytic asymmetric Nazarov reactions of N-heterocycles. See ref 2j.

(9) For a review of asymmetric electrocyclic reactions, see: Thompson, S.; Coyne, A. G.; Knipe, P. C.; Smith, M. D. *Chem. Soc. Rev.* **2011**, *40*, 4217–4231.

(10) (a) Okino, T.; Hoashi, Y.; Takemoto, Y. *J. Am. Chem. Soc.* **2003**, *125*, 12672–12673. (b) Schreiner, P. R. *Chem. Soc. Rev.* **2003**, *32*, 289–296. (c) Takemoto, Y. *Org. Biomol. Chem.* **2005**, *3*, 4299–4306. (d) Connon, S. J. *Chem. - Eur. J.* **2006**, *12*, 5418–5427. (e) Taylor, M. S.; Jacobsen, E. N. *Angew. Chem., Int. Ed.* **2006**, *45*, 1520–1543. (f) Doyle, A. G.; Jacobsen, E. N. *Chem. Rev.* **2007**, *107*, 5713–5743. (g) Connon, S. J. *Chem. Commun.* **2008**, 2499–2510. (h) Yu, X.; Wang, W. *Chem. - Asian J.* **2008**, *3*, 516–532. (i) Zhang, Z.; Schreiner, P. R. *Chem. Soc. Rev.* **2009**, *38*, 1187–1198. (j) Cheong, P. H.-Y.; Legault, C. Y.; Um, J. M.; Çelebi-Ölçüm, N.; Houk, K. N. *Chem. Rev.* **2011**, *111*, 5042–5137. (k) Siau, W.-Y.; Wang, J. *Catal. Sci. Technol.* **2011**, *1*, 1298–1310. (l) Lu, L.-Q.; An, X.-L.; Chen, J.-R.; Xiao, W.-J. *Synlett* **2012**, *23*, 490–508. (m) Serdyuk, O. V.; Heckel, C. M.; Tsogoeva, S. B. *Org. Biomol. Chem.* **2013**, *11*, 7051–7071. (n) Zhang, Z.; Bao, Z.; Xing, H. *Org. Biomol. Chem.* **2014**, *12*, 3151–3162.

(11) Frisch, M. J.; Trucks, G. W.; Schlegel, H. B.; Scuseria, G. E.; Robb, M. A.; Cheeseman, J. R.; Scalmani, G.; Barone, V.; Mennucci, B.; Petersson, G. A.; Nakatsuji, H.; Caricato, M.; Li, X.; Hratchian, H. P.; Izmaylov, A. F.; Bloino, J.; Zheng, G.; Sonnenberg, J. L.; Hada, M.; Ehara, M.; Toyota, K.; Fukuda, R.; Hasegawa, J.; Ishida, M.; Nakajima, T.; Honda, Y.; Kitao, O.; Nakai, H.; Vreven, T.; Montgomery, J. A., Jr.; Peralta, J. E.; Ogliaro, F.; Bearpark, M.; Heyd, J. J.; Brothers, E.; Kudin, K. N.; Staroverov, V. N.; Keith, T.; Kobayashi, R.; Normand, J.;

Raghavachari, K.; Rendell, A.; Burant, J. C.; Iyengar, S. S.; Tomasi, J.; Cossi, M.; Rega, N.; Millam, J. M.; Klene, M.; Knox, J. E.; Cross, J. B.; Bakken, V.; Adamo, C.; Jaramillo, J.; Gomperts, R.; Stratmann, R. E.; Yazyev, O.; Austin, A. J.; Cammi, R.; Pomelli, C.; Ochterski, J. W.; Martin, R. L.; Morokuma, K.; Zakrzewski, V. G.; Voth, G. A.; Salvador, P.; Dannenberg, J. J.; Dapprich, S.; Daniels, A. D.; Farkas, O.; Foresman, J. B.; Ortiz, J. V.; Cioslowski, J.; Fox, D. J. *Gaussian 09*, Rev. D.01; Gaussian, Inc.: Wallingford, CT, 2013.

(12) (a) Zhao, Y.; Truhlar, D. *Theor. Chem. Acc.* **2008**, *120*, 215–241. (b) Zhao, Y.; Truhlar, D. G. *Acc. Chem. Res.* **2008**, *41*, 157.

(13) Weigend, F.; Ahlrichs, R. *Phys. Chem. Chem. Phys.* **2005**, *7*, 3297–3305.

(14) (a) Ribeiro, R. F.; Marenich, A. V.; Cramer, C. J.; Truhlar, D. G. *J. Phys. Chem. B* **2011**, *115*, 14556–14562. (b) Zhao, Y.; Truhlar, D. G. *Phys. Chem. Chem. Phys.* **2008**, *10*, 2813–2818.

(15) (a) Howard, D. L.; Kjaergaard, H. G. *J. Phys. Chem. A* **2006**, *110*, 10245–10250. (b) Lane, J. R.; Contreras-García, J.; Piquemal, P.; Miller, B. J.; Kjaergaard, H. G. *J. Chem. Theory Comput.* **2013**, *9*, 3263–3266.

(16) (a) Jefford, C. W.; Bernardinelli, G.; Wang, Y.; Spellmeyer, D. C.; Buda, A.; Houk, K. N. *J. Am. Chem. Soc.* **1992**, *114*, 1157–1165. (b) Nakamura, K.; Houk, K. N. *J. Org. Chem.* **1995**, *60*, 686–691. (c) Dolbier, W. R.; Koroniak, H.; Houk, K. N. *Acc. Chem. Res.* **1996**, *29*, 471–477.

(17) Kallef, E. A.; Houk, K. N. *J. Org. Chem.* **1989**, *54*, 6006–6008.

(18) (a) Sayer, J. M.; Jencks, W. P. *J. Am. Chem. Soc.* **1973**, *95*, 5637. (b) Rosenberg, S.; Silver, S. M.; Sayer, J. M.; Jencks, W. P. *J. Am. Chem. Soc.* **1974**, *96*, 7986. (c) Sayer, J. M.; Pinsky, B.; Schonbrunn, A.; Washien, W. *J. Am. Chem. Soc.* **1974**, *96*, 7998. (d) Kayser, R. H.; Pollack, R. M. *J. Am. Chem. Soc.* **1977**, *99*, 3379. (e) Sayer, J. M.; Conlon, P. J. *Am. Chem. Soc.* **1980**, *102*, 3592. (f) Yamataka, H.; Nagase, S.; Ando, T.; Hanafusa, T. *J. Am. Chem. Soc.* **1986**, *108*, 601. (g) Hall, N. E.; Smith, B. J. *J. Phys. Chem. A* **1998**, *102*, 4930. (h) Pliego, J. R., Jr.; Alcantara, A. F. C.; Veloso, D. P.; Almeida, W. B. *J. Braz. Chem. Soc.* **1999**, *10*, 381. (i) Mascavage, L. M.; Sonnet, P. E.; Dalton, D. R. *J. Org. Chem.* **2006**, *71*, 3435. (j) Evans, G. J. S.; White, K.; Platts, J. A.; Tomkinson, N. C. O. *Org. Biomol. Chem.* **2006**, *4*, 2616. (k) Patil, M. P.; Sunoj, R. B. *J. Org. Chem.* **2007**, *72*, 8202–8215.

(19) Plata, R. E.; Singleton, D. A. *J. Am. Chem. Soc.* **2015**, *137*, 3811–3826.

(20) Bow, W. F.; Basak, A. K.; Jolit, A.; Vivic, D. A.; Tius, M. A. *Org. Lett.* **2010**, *12*, 440–443.

(21) Hamza, A.; Schubert, G.; Soós, T.; Pápai, I. *J. Am. Chem. Soc.* **2006**, *128*, 13151–13160.

(22) Moss, G. P. *Pure Appl. Chem.* **1996**, *68*, 2193–2222.

(23) See [Supporting Information](#) for details.

(24) (a) Jorgensen, W. L.; Pranata, J. *J. Am. Chem. Soc.* **1990**, *112*, 2008–2010. (b) Pranata, J.; Wierschke, S. G.; Jorgensen, W. L. *J. Am. Chem. Soc.* **1991**, *113*, 2810–2819.